All-optical format conversion of NRZ-OOK to QPSK and 16QAM signals via XPM in a SOA-MZI

Yueying Zhan (展月英)*, Min Zhang (张 民), Mintao Liu (刘明涛), Lei Liu (刘 磊), and Xue Chen (陈 雪)

State Key Laboratory of Information Photonics and Optical Communications, Beijing University of Posts and Telecommunications, Beijing 100876, China

**Corresponding author: zhanyueying@gmail.com*

Received September 4, 2012; accepted November 16, 2012; posted online February 28, 2013

This letter proposes a scheme for the format conversion of on-off keying (OOK) signal to quadrature phase-shift keying (QPSK) and 16-ary quadrature amplitude modulation (16QAM) signals via cross-phase modulation (XPM) in a semiconductor optical amplifier (SOA). Theoretical and experimental analyses of the format conversion scheme are conducted to validate its feasibility. The phase changing is obtained because of the XPM in the SOA. The QPSK and 16QAM signals are converted from the OOK signal. The performance of the 10 Gb/s format conversion system is evaluated and discussed. The receiver sensitivities of the converted QPSK and 16QAM signals after detection are –27.25 and –23.5 dBm, respectively, at a bit error rate (BER) of 10^{-9}.

OCIS codes: 060.2330, 230.4480, 070.4340.
doi: 10.3788/COL201311.030604.

All-optical signal processing is a promising technology for future optical transparent networks because it helps reduce implementation costs and removes the bottleneck in ultrafast signal processing without requiring costly optical-electrical-optical equipment[1,2]. Optical format conversion, one of the key optical signal processing technologies, has been extensively studied. Researchers have mainly focused on the conversion between conventional on-off keying (OOK) and binary phase shift keying (BPSK)[3–6]. By contrast, the multiple-OOK to M-ary phase-shift keying and/or quadrature amplitude modulation (QAM) conversion is rarely demonstrated. The OOK to BPSK conversion can be conducted in commercially available semiconductor optical amplifier (SOA) because of the simplicity of the BPSK format. However, the conversion of multiple OOK signals to higher order constellation signals is more difficult to achieve and requires a more flexible device approach than that of a single SOA. Based on previous reports, schemes are usually complex and costly, such as cascaded Mach–Zehnder modulators (MZMs) followed by a phase modulator[7], dual-parallel MZM[8], dual-drive MZM[9], and parallel SOA Mach-Zehnder interferometer (MZI)[10].

In this letter, a novel scheme for the format conversion of nonreturn to zero (NRZ)-OOK signal to QPSK or 16-ary QAM (16QAM) signal via cross-phase modulation (XPM) in a SOA based MZI (SOA-MZI) is proposed and verified. The return to zero (RZ) pulse and dual NRZ-OOK signals are injected into a SOA, and the quadrature phase-shift keying (QPSK) signal is converted from an OOK signal via the XPM in the SOA. The dual NRZ-OOK signals are then injected into the SOAs located at the upper and lower MZI arm. Therefore, the dual QPSK signal is converted at the lower and upper arm via the XPM in the SOA-MZI. The 16QAM signal can then be converted by coupling the double QPSK signals. The scheme is simpler, more compact, and cost-efficient than traditional schemes. Our format conversion scheme is entirely in the optical domain and reduces the unstable factors in the electrical domain. The feasibility of this technique is evaluated through theoretical and experimental analyses.

Figure 1 shows the theoretical analysis of the format conversion based on the XPM effect in a SOA[11]. Two NRZ-OOK signals with wavelengths λ_1 and λ_2 and a RZ clock pulse signal with wavelength λ_3 were injected into the SOA. The OOK signals modulate the SOA gain by depleting the carriers, thereby changing the refractive index and phase of the RZ clock pulse signal. The SOA was divided into a number of smaller sections to analyze the carrier change in the SOA. The rate equation of the carrier density is given by[11]

$$\frac{\mathrm{d}N_i}{\mathrm{d}t} = \frac{J}{qd} - \frac{N_i}{\tau_i} - \sum_{x=1,2,3} \frac{g_{\mathrm{m}_i}^{(x)} I_i^{(x)}}{E^{(x)}} - g_{\mathrm{m_p}} S_{\mathrm{t}_i}, \quad (1)$$

where N is the carrier density, J is the injection current density, d is the active layer thickness, τ is the carrier life time, g_{m} is the material gain, i is the ith section of the SOA, index x refers to the different optical input (NRZ-OOK1 signal, NRZ-OOK2 signal, and RZ clock pulse signal), g_{mp} is the value at peak gain wavelength, S_{t_i} is the average amplified spontaneous emission in section i, E is the photon energy, and I is the injection light intensity.

The nonlinear phase change, arising from the carrier density-induced changes in the refractive index, is given by[10,11]

$$\phi_i = \frac{2\pi L}{\lambda_\omega}\left(N_{\mathrm{r}} + \Gamma \mathrm{n_p}\frac{\mathrm{d}N}{\mathrm{d}n}\right) + \frac{2\pi L_i(n_i - n_0)}{\lambda_\omega}\frac{\mathrm{d}N}{\mathrm{d}n} = \frac{\pi \Delta L g_{\mathrm{m}_i}}{2a_1\lambda_\omega}\Delta\overline{n}_{\mathrm{N}}, \quad (2)$$

where Γ is the optical confinement factor, L_i is the cavity

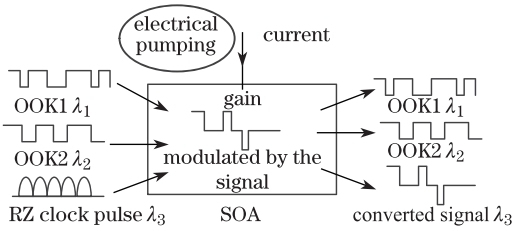

Fig. 1. Conversion process of electrical signals to optical signals in a SOA.

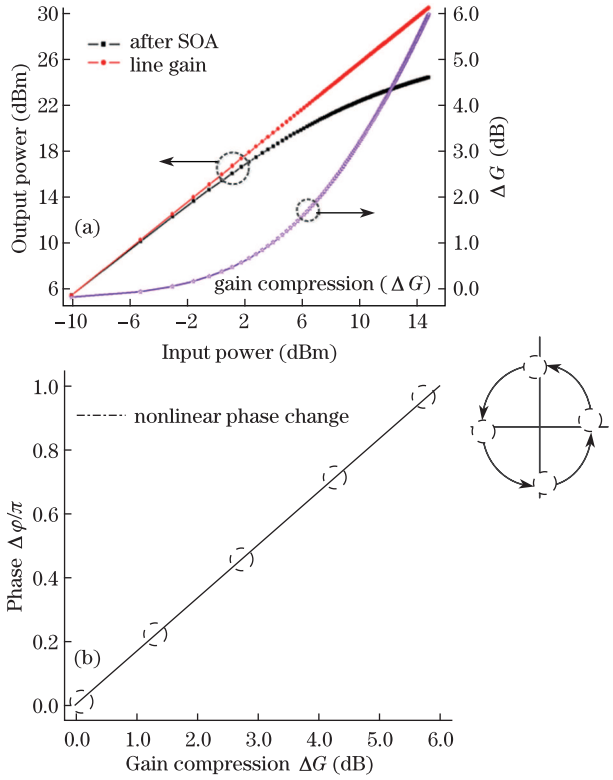

Fig. 2. Gain and phase change curves after the SOA. (a) The curves of the output after the SOA and line gains, as well as the curves of the gain compression between the output signals; (b) nonlinear phase changes with gain compression.

length, n_0 is the transparency carrier concentration, λ_ω is the beam wavelength, N_r is the guide refractive index, and n_p is the value of the carrier concentration for zero input at the bias current used to define the peak wavelength. $\mathrm{d}N/\mathrm{d}n$ is the rate of change of the active region refractive index with carrier concentration, which is affected by the gain compression of the SOA. Therefore, the nonlinear phase change is related to the gain compression, which was also discussed in Ref. [12]. The gain compression curve and relationship between the output and input powers of the SOA are shown in Fig. 2(a). Figure 2(b) depicts the nonlinear phase change with SOA gain compression. The gain compression is determined by the input signal power; therefore, the power of the input signals should be suitably controlled in our system. Based on the result, the phase changes are "0" when the gain compression is at the minimum value, "π" when the gain compression is at the maximum value, and "$\pi/2$" when the gain compression is half of the maximum value.

Figure 3 shows the schematic of the proposed modulation format converter. The QPSK signal was converted from the OOK signal based on the scheme shown in Fig. 3(a). The 16QAM signal can be converted based on the scheme shown in Fig. 3(b). Dual NRZ-OOK signals with wavelengths λ_1 and λ_2, as control signals, and a RZ clock pulse with wavelength λ_3 as the probe signal were mixed and fed into the SOA. When the NRZ-OOK1 and NRZ-OOK2 data are "1" or "0" at the same time, the SOA gain compression obtained is the maximum or minimum value. The RZ clock pulse signal after passing through the SOA has the phase "π" or "0" because of the carrier density changes. On the contrary, when the NRZ-OOK1 data is "1", and the NRZ-OOK2 data is "0", the gain compression is half of the maximum value, and the phase of the clock pulse is "$\pi/2$". However, when the NRZ-OOK1 data is "0" and the NRZ-OOK2 data is "1", the phase of clock pulse is "$-\pi/2$". Therefore, the QPSK signal can be converted from the OOK signal based on the XPM effect in the SOA. The 16QAM signal can then be converted via the superposition of the two QPSK signals. The amplitude of QPSK2 is doubled compared with QPSK1[9,13], as expressed by

$$\begin{pmatrix} E_{16\mathrm{QAM}} \\ E_{2,\mathrm{ut}} \end{pmatrix} = \begin{pmatrix} \sqrt{1-\alpha} & \mathrm{j}\sqrt{\alpha} \\ \mathrm{j}\sqrt{\alpha} & \sqrt{1-\alpha} \end{pmatrix} \cdot \begin{pmatrix} E_{\mathrm{QPSK1}} \\ E_{\mathrm{QPSK2}} \end{pmatrix}, \tag{3}$$

$$\begin{aligned} E_{16\mathrm{QAM}}(t) = \frac{\sqrt{2}}{2} A \Big\{ \Big[& \cos\theta_1 \cos(2\pi f_\mathrm{c} t) \\ & + \frac{1}{2} \sin\theta_2 \sin(2\pi f_\mathrm{c} t) \Big] \\ & + \mathrm{j}\Big[\frac{1}{2} \cos\theta_2 \cos(2\pi f_\mathrm{c} t) \\ & - \sin\theta_1 \sin(2\pi f_\mathrm{c} t) \Big] \Big\}, \end{aligned} \tag{4}$$

where the value of α is 0.5, which is the couple index of the coupler, θ_i is the phase value of the QPSK$_i$($i = 1, 2$) and f_c is the frequency of the QPSK$_i$ signals. The phase values of the QPSK signal were assumed as $\frac{\pi}{4}$, $\frac{3\pi}{4}$, $\frac{5\pi}{4}$, and $\frac{7\pi}{4}$. Thus, the 16QAM signal has three different amplitude values and twelve different phase values.

The experimental setup of the format converter for the conversion of OOK signal to the QPSK and 16QAM signals are shown in Figs. 4(a) and (b). The NRZ-OOK1 and NRZ-OOK2 signals were generated by modulating the continuous wave (CW) light at λ_{OOK1}=1 556 nm and λ_{OOK2}=1 554 nm in a lithium niobate ($LiNbO_3$)

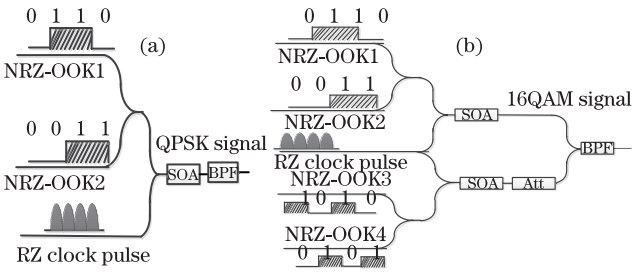

Fig. 3. Schematic of the proposed format conversion. Converted (a) QPSK and (b) 16QAM signals. PS: phase shifter, Att: attenuator, BPF: band pass filter.

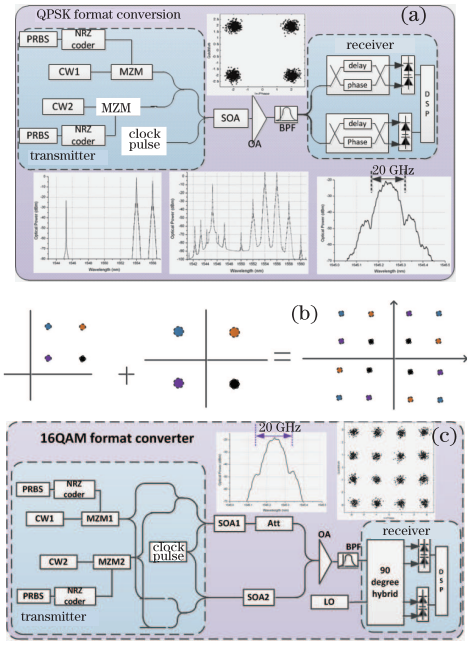

Fig. 4. Experimental setup of the QPSK and 16QAM signals. (a) QPSK format converter, (b) conceptual diagram of constellation mapping, and (c) 16QAM format converter. PRBS: pseudo-random binary sequence, LO: local oscillator, OA: optical amplifier, DSP: digital signal processing.

modulator with a 10-Gbps bit stream and a pseudo random binary sequence (PRBS) of 2^{11}–1. The wavelength of the RZ clock pulse signal is 1 545.2 nm. The average powers of the OOK1, OOK2, and clock pulse signals are –5.4, 8.9, and –5.87 dBm, respectively. The OOK1, OOK2, and clock pulse signals were injected into the SOA. The OOK signals were converted into QPSK signals because of the XPM effect in the SOA. The optical spectra before and after the SOA are shown in Fig. 4(a), which also shows the spectra and constellations of the converted QPSK signal. The mainlobe bandwidth is approximately 20 GHz. The constellation points of the 16QAM signal in the I/Q plane can be determined by the offset QPSK1 distribution, whereas the second QPSK determines the phase rotation of the offset QPSK1 constellation points in four different quadrants[14]. The four NRZ-OOK signals and RZ clock pulse were injected into the upper and lower SOA of the MZI, as shown in Fig. 4(c). Thus, the two QPSK signals were converted at the upper and lower arms of the SOA-MZI. The attenuator located at the upper arm of the MZI was set at 6 dB, and the amplitude ratio of the two QPSK signals was set as 0.5. Therefore, the 16QAM signal was converted after the QPSK signals coupled via a 3-dB coupler. The spectra and constellation are shown in Fig. 4(c). Furthermore, the mainlobe bandwidth of the converted 16QAM signal was about 20 GHz. In the receiver, the received signal after balanced was detected is processed offline. The CW light of the emitter-coupled logic was used as the local oscillator, providing self-homodyne detection and avoiding the need for frequency offset estimation between the transmitter and local oscillator. The received electrical signal was converted from an analog-to-digital signal using an oscilloscope and processed offline to perform normalization, carrier-phase estimation symbol detection, and bit error rate (BER) estimation[15].

Figure 5 presents the effect of bias current on the performance of the conversion scheme at different RZ clock pulse powers. From the rate equation of the carrier density, which is expressed as Eq. (1), the carrier density change in SOA decreases with increasing current and further influences the refractive index. Therefore, as the bias current increases, the BER performance of the converted QPSK signal decreases at different clock pulse powers. When the bias current is lower than 0.35 A, the performance increases with decreasing RZ clock pulse input power. However, the performance is better when the RZ clock power is higher at a bias current higher than 0.35 A. In our system, the bias current of the SOA was set to 0.25 A for error free operation.

Based on above discussions on the SOA parameters, the BER of the converted QPSK signal under different fiber transmissions are shown in Fig. 6. The generated QPSK signal was received via direct detection combined with the delay interference and balanced detection, as shown in Fig. 4(a). The power penalties of 2.25 and 3.5 dB at a BER of 10^{-9} were obtained after 20- and 40-km fiber transmissions. The respective receiver sensitivities of the QPSK signal were –25 and –23.75 dBm. The BER performance of the QPSK signal after fiber transmission ranged from 10 to 100 km (Fig. 7). The BER of the proposed system was degraded with the extension of the fiber link because of the time shifting effect induced by cumulated chromatic dispersion.

In our system, the 16QAM signal was converted by the coupling of two QPSK signals. The amplitude of QPSK1 was twice that of the other QPSK signal, as depicted by Fig. 4(b). Figure 8 shows the BER performance

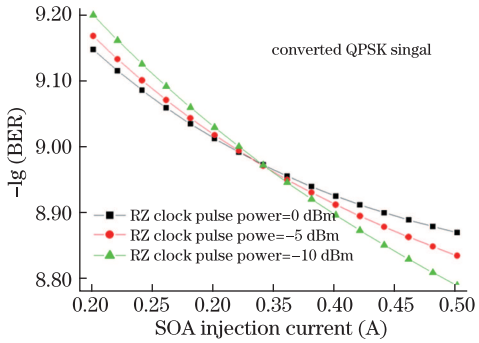

Fig. 5. Received BER of the converted QPSK signal versus the SOA bias current.

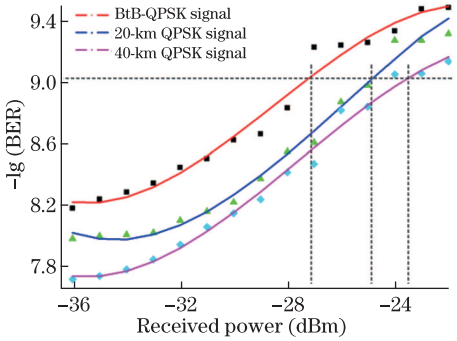

Fig. 6. Measured back-to-back (BtB) BER of the QPSK signal with different fiber transmissions.

of 16QAM with 20- and 40-km back-to-back (BtB) fiber transmissions at the power penalties of 1.25 and 2.6 dB, respectively. The receiver sensitivity of the converted 16QAM signal after detection was –23.5 dBm at a BER of 10^{-9}. The BER performance of the converted 16QAM signal after fiber transmission ranged from 10 to 100 km (Fig. 9). The BER of the proposed system was degraded with the extension of the fiber link because of the time shifting effect induced by cumulated chromatic dispersion.

In conclusion, we propose a scheme for the format conversion of OOK to QPSK and 16QAM via XPM in a SOA-MZI. The scheme is theoretically analyzed and experimentally verified. The optimal injection current of the SOA is also explored, and the transmission performances of the converted QPSK and 16QAM signals are experimentally investigated. The BtB receiver sensitivities of the converted QPSK and 16QAM signals after detection are –27.25 and –23.5 dBm, respectively, at a BER of 10^{-9}. Further optimization of system parameters can improve the performance of the proposed format conversion technology.

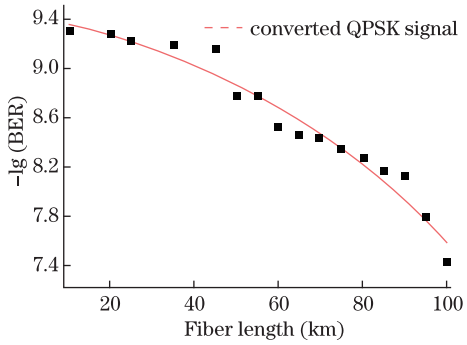

Fig. 7. Received BER of the QPSK signal versus fiber length.

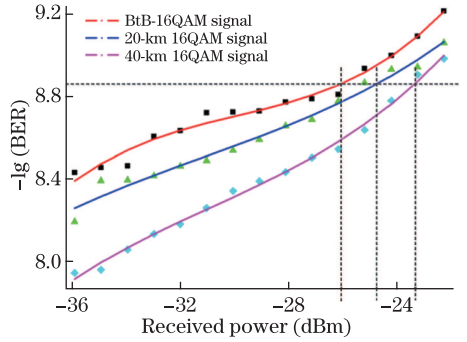

Fig. 8. (Color online) BER of the 16QAM signal with different fiber transmissions.

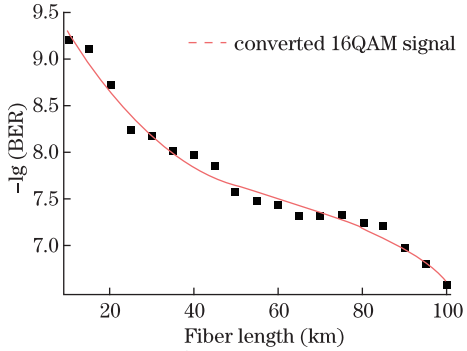

Fig. 9. BER of 16QAM signal versus fiber length.

This work was supported by the National Natural Science Foundation of China (No. 61072008), the National "863" Project of China (No. 2012AA011302), the Fundamental Research Funds for Central Universities (Nos. 2009GYBZ and 2009RC0401), and the Beijing Municipal Education Commission Science and Technology Programs (Nos. KM200610009014 and KM201110009001).

References

1. X. Zhou and J. Yu, J. Lightwave Technol. **27,** 3641 (2009).
2. P. J. Winzer and R.-J. Essiambre, J. Lightwave Technol. **24,** 4711 (2006).
3. H. Jiang, H. Wen, L. Han, Y. Guo, and H. Zhang, IEEE Photon. Technol. Lett. **19,** 1985 (2007).
4. C. Yan, Y. Su, L. Yi, L. Leng, X. Tian, X. Xu, and Y. Tian, IEEE Photon. Technol. Lett. **18,** 2368 (2006).
5. W. Astar and G. M. Carter, Electron. Lett. **44,** 369 (2008).
6. W. Astar, P. Apiratikul, B. M. Cannon, T. Mahmood, J. J. Wathen, J. V. Hryniewicz, S. Kanakaraju, C. J. K. Richardson, T. E. Murphy, and G. M. Carter, IEEE Photon. Technol. Lett. **23,** 1397 (2011).
7. M. Seimetz, in *Proceedings of 2005 7th International Conference on Transparent Optical Networks* (*ICTON*) **2,** 225 (2005).
8. T. Kawanishi, T. Sakamoto, A. Chiba, M. Izutsu, K. Higuma, J. Ichikama, T. Lee, and V. Filsinger, in *Proceedings of Optical Fiber Communication Conference and Exposition and the National Fiber Optic Engineers Conference* (*OFC/NFOEC*) JThA34 (2008).
9. M. Nakamura, Y. Kamio, and T. Miyazaki, in *Proceedings of Optical Fiber Communication Conference and Exposition and the National Fiber Optic Engineers Conference* (*OFC/NFOEC*) JThA042 (2011).
10. K. Mishina, S. M. Nissanka, A. Maruta, S. Mitani, K. Ishida, K. Shimizu, T. Hatta, and K.-I. Kitayama, Opt. Express **15,** 7774 (2007).
11. M. Asghari, I. H. White, and R. V. Penty, J. Lightwave Technol. **15,** 1181 (1997).
12. H. J. Lee, M. Sohn, K. Kim, and H. G. Kim, IEEE Photon. Technol. Lett. **11,** 185 (1999).
13. G. Huang, Y. Miyoshi, Y. Yoshida, A. Maruta, and K.-I. Kitayama, in *Proceedings of Optical Fiber Communication Conference and Exposition and the National Fiber Optic Engineers Conference* (*OFC/NFOEC*) OTh4H.3 (2012).
14. Z. Bakhtiari, R. Hellwarth, and A. Willner, in *Proceedings of Optical Fiber Communication Conference and Exposition and the National Fiber Optic Engineers Conference* (*OFC/NFOEC*) JW2A.87 (2012).
15. S. Yan, D. Wang, Y. Gao, C. Lu, A. P. T. Lau, L. Liu, and X. Xu, in *Proceedings of Optical Fiber Communication Conference and Exposition and the National Fiber Optic Engineers Conference* (*OFC/NFOEC*) OW3H.3 (2012).